

Supporting Information for

Gold Nanoparticle-Based Activatable Probe for Sensing Ultra-Low Levels of Prostate-Specific Antigen

*Dingbin Liu,¹ Xinglu Huang,¹ Zhantong Wang,² Albert Jin,³ Xiaolian Sun,¹ Lei Zhu,^{1,2} Fu Wang,¹
Ying Ma,¹ Gang Niu,¹ Angela R. HightWalker,⁴ and Xiaoyuan Chen^{2*}*

1. Laboratory of Molecular Imaging and Nanomedicine, National Institute of Biomedical Imaging and Bioengineering, National Institutes of Health, Bethesda, Maryland 20892 (United States)

2. Center for Molecular Imaging and Translational Medicine, School of Public Health, Xiamen University, Xiamen 361005 (China)

3. Laboratory of Cellular Imaging and Macromolecular Biophysics, National Institute of Biomedical Imaging and Bioengineering, National Institutes of Health, Bethesda, Maryland 20982 (United States)

4. Optical Technology Division, Physics Laboratory, National Institute of Standards and Technology, Gaithersburg, Maryland 20899 (United States)

** To whom correspondence should be addressed.*

E-mail: Xiaoyuan Chen (shawn.chen@nih.gov)

Table S1 Spectral characteristics of the AuNPs used in this report

Particle diameter (nm)	Maximum absorption (nm)	Extinction coefficient, ϵ ($M^{-1} cm^{-1}$)
15	520	3.64×10^8
30	525	3.58×10^9
60	540	3.53×10^{10}
80	553	9.12×10^{10}

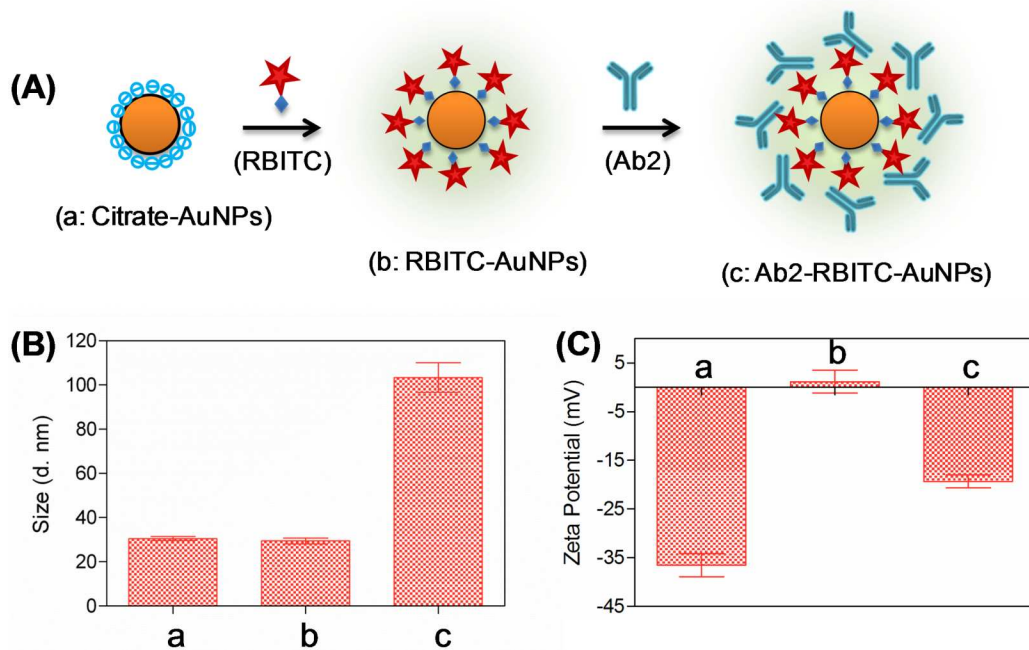


Figure S1. (A) Procedure of preparing Ab2-RBITC-AuNPs. (B) DLS and (C) zeta potentials measurements of citrate-AuNPs (a), RBITC-AuNPs (b), and Ab2-RBITC-AuNPs (c). **Error bars show standard deviations (n=3).**

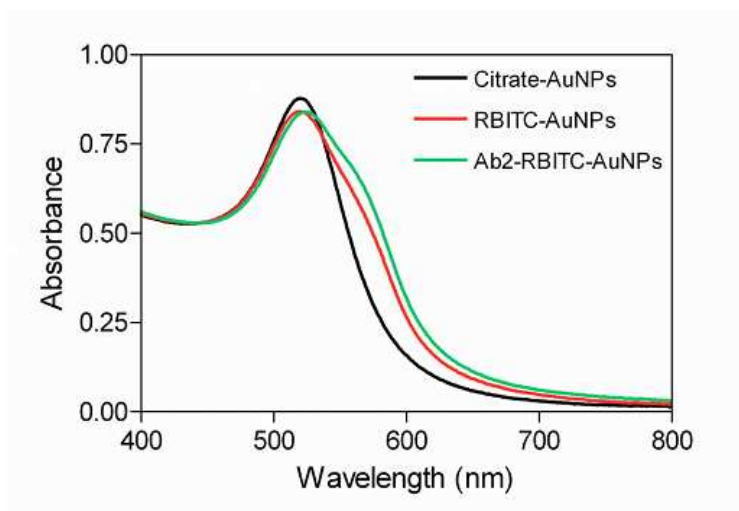


Figure S2. Absorption spectra of citrate-AuNPs, RBITC-AuNPs, and Ab2-RBITC-AuNPs where the particle size is 15 nm.

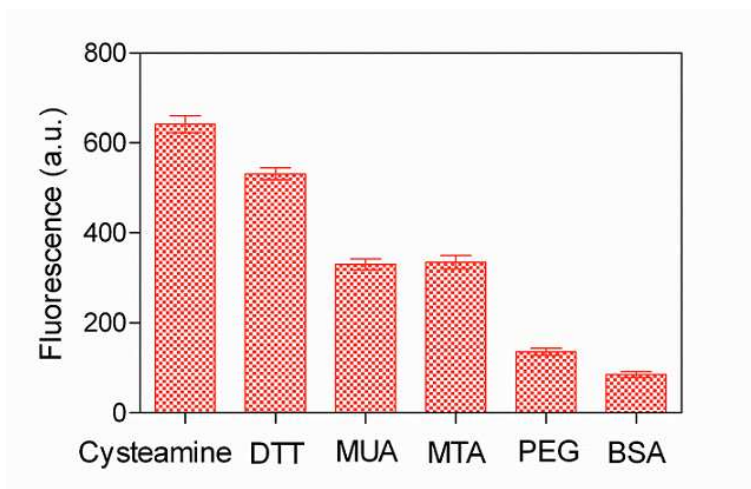


Figure S3. Fluorescence intensities of Ab2-RBITC-AuNPs solutions in the presence of various kinds of thiol-contained compounds (1 mM for each compound). Error bars show standard deviations (n=3).

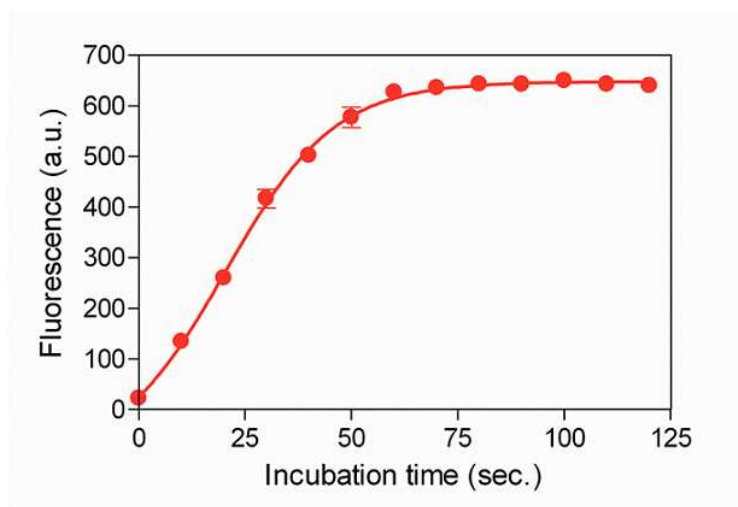


Figure S4. Fluorescence intensities of Ab2-RBITC-AuNPs solutions versus incubation time after addition of 1 mM cysteamine into Ab2-RBITC-AuNPs solutions. Error bars show standard deviations (n=3).

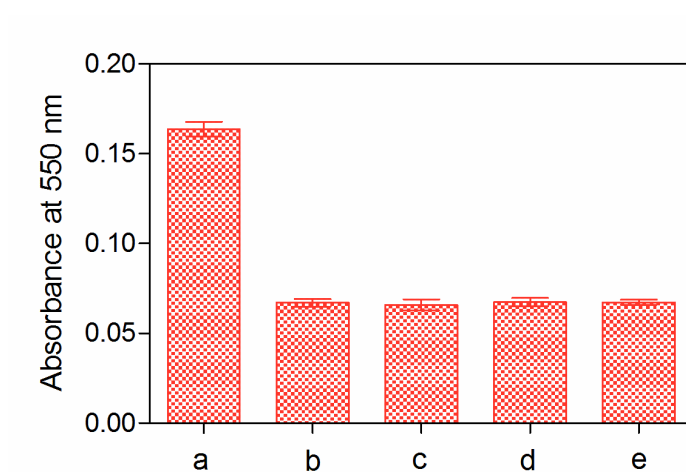


Figure S5. Absorbance of free RBITC at 550 nm before (a) and after attaching onto surfaces of AuNPs with diameters of 15 (b), 30 (c), 60 (d), and 80 nm (e), respectively. The total surface area for each size of AuNP solution is the same. Error bars show standard deviations (n=3).

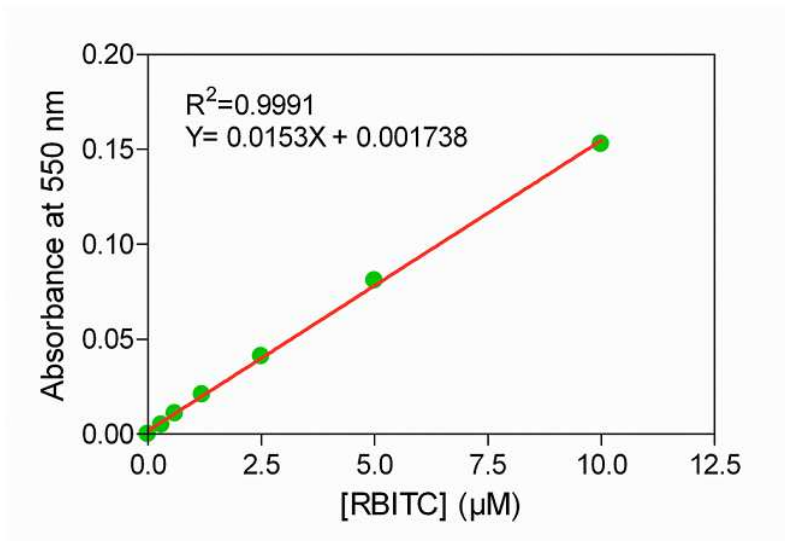


Figure S6. Plot of absorbance at 550 nm versus varying concentrations of RBITC from 0.3 to 10 µM.

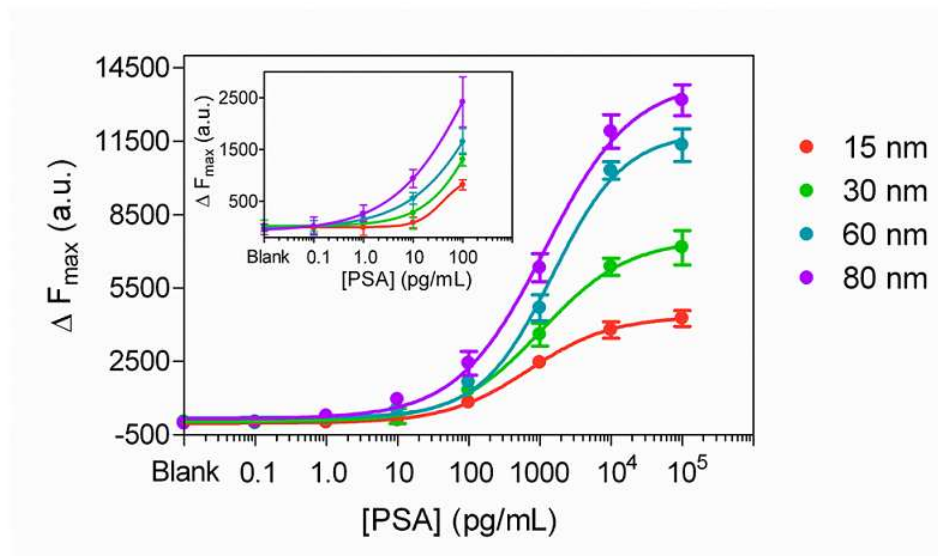


Figure S7. Plots of ΔF_{\max} values generated by the immobilized Ab2-RBITC-AuNPs with diameters of 15, 30, 60, and 80 nm versus varying concentrations of PSA from 0.1 pg/mL to 100 ng/mL. The PBST-only sample was set as the blank. The fluorescence intensities were collected by a Synergy 2 Multi-Mode Microplate Reader using 530 nm excitation wavelength and 590 nm emission wavelength. **Error bars show standard deviations (n=3).**

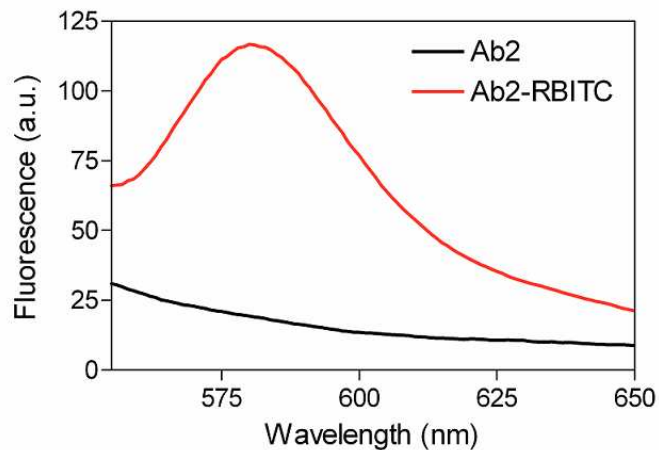


Figure S8. Fluorescence emission spectra of 100 ng/mL of Ab2 and Ab2-RBITC in de-ionized water using 530 nm excitation wavelength.

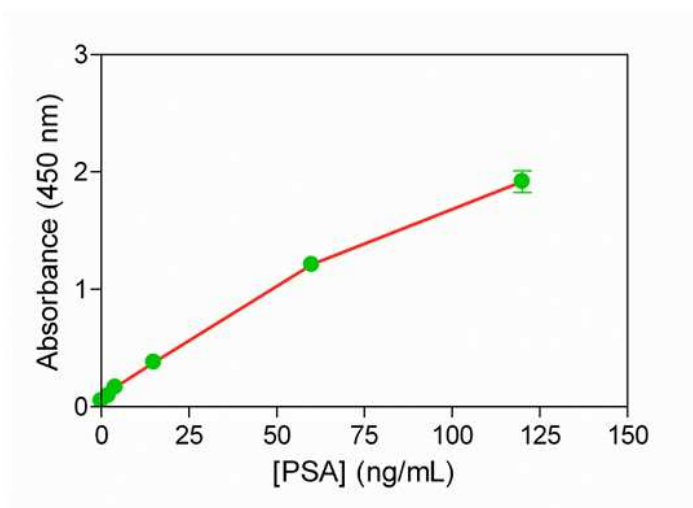


Figure S9. Commercially available HRP-based immunoassays for sensing varying concentrations of PSA from 1 to 120 ng/mL used as a standard curve. **Error bars show standard deviations (n=3).**